

FOURTEENTH EUROPEAN ROTORCRAFT FORUM

Paper No. 10

WINGLETS ON ROTORBLADES IN FORWARD FLIGHT  
- A THEORETICAL AND EXPERIMENTAL INVESTIGATION

R. H. G. Müller

Paul Klee Weg 8  
D-4000 Düsseldorf, F. R. Germany

September 20 - 23, 1988

MILANO, ITALIA

ASSOCIAZIONE INDUSTRIE AEROSPAZIALI  
ASSOCIAZIONE ITALIANA DI AERONAUTICA ED ASTRONAUTICA

## NOTATION

$r$	:	Radius
$r_k$	:	Vortex core radius
$R$	:	Rotor radius
$v_t$	:	tangential velocity in vortex core
$\beta$	:	Angle of tip path plane
$\beta_M$	:	Angle between microphone and tip path plane (negative downward)
$\alpha$	:	Angle of attack (2-dimensional theory)
$\alpha_a$	:	Angle of attack at blade tip
$\Gamma$	:	Circulation
$\alpha_m$	:	Mean angle of attack (cyclic)
$\alpha_{90^\circ}$	:	Angle of attack (advancing blade)
$\alpha_{270^\circ}$	:	Angle of attack (retreating blade)
$\mu$	:	Advance ratio ( $v_{00} / (\omega r)$ )
$\psi$	:	Azimuth of rotor
$\psi_M$	:	Azimuth of microphone
$\omega$	:	Rotor speed

# WINGLETS ON ROTORBLADES IN FORWARD FLIGHT A THEORETICAL AND EXPERIMENTAL INVESTIGATION

Reinert H. G. Müller

## ABSTRACT

While several investigations have shown the favourable influence of downward pointing winglets on rotor aerodynamics in hover flight there has still been the question of winglet behaviour in forward flight. This paper presents a discussion of the influence of an optimized winglet arrangement on the rotor aerodynamics under forward flight conditions. Using combined experimental and theoretical methods it will be evident that there are advantages of winglets even in forward flight. Up to high values of the advance ratio the influence of blade-vortex-interactions (BVI) could be decreased considerably. This results in lower blade stress and lower noise emission. However, problems occur at high advance ratio on the winglet itself due to the variation of the angle of attack produced by the forward flight speed.

## 1. INTRODUCTION

Interactions of tip vortices with rotorblades are known to have an adverse influence on rotor aerodynamics. These blade-vortex-interactions (BVI) result in large unsteady induced velocities on the blades (Fig. 1), causing unsteady pressure fluctuations, blade stress and noise emission. It could be shown /1/, that special winglet arrangements with downward pointing winglets at the blade tips result in a vertical displacement (Fig. 2) and a diffuse core of the tip vortex, leading to lower induced velocities at BVI (Fig. 3). While the results presented in reference /1/ show the influence of preliminary winglet versions, this paper will briefly discuss the influence of an optimized winglet under forward flight conditions. A more detailed explanation and additionally a closer look at the advantages of the same optimized winglet shape in hover flight conditions will be published in reference /2/.

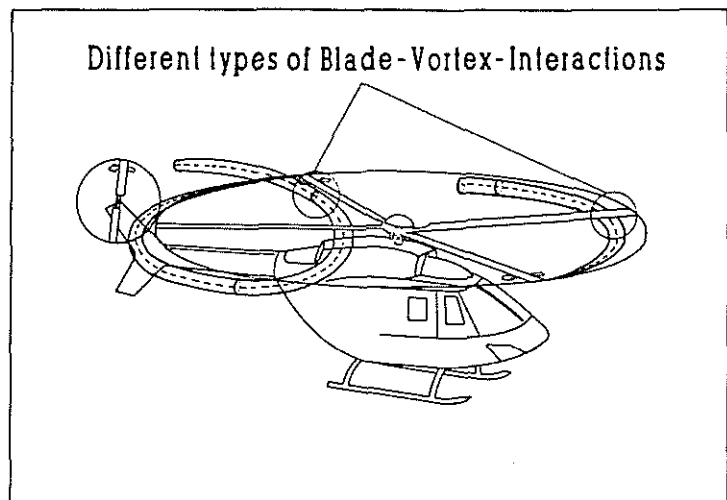


Fig. 1 Blade-Vortex-Interactions

The winglet arrangement used is shown in Fig. 4. Several demands led to this relatively exotic looking shape. First of all it was necessary to form a very smooth downward bending. This reduces the danger of aerodynamic losses by disturbances like secondary vortices or flow separation. This is very important in forward flight conditions, because of the very large variations the angle of attack can have on the

outer winglet part. The sweep angle gives a good behaviour at transonic velocities, which occur at the  $\psi = 90^\circ$  position. According to Desopper /3/ there is a decreasing effect on the effective sweep angle in the second quadrant ( $\psi = 90^\circ$  to  $180^\circ$ ). It is important to notice that this effect is -- due to the special bent down shape of the winglet -- almost completely eliminated. To reduce the torsional forces produced by the swept back part there is a small forward swept part just at the start of the downward bending. Due to the centrifugal forces on the winglet there is a large blade stress at the bending. A given limit of the blade stress requires a large thickness in this region, which interferes with the demand of thin profiles for transonic tip speeds. Therefore a relatively thin airfoil with a wide chord has been chosen, which results in a good compromise and has advantages even at the retreating side of the rotor. The twist of the outer winglet part determines the amount of circulation on the winglet,

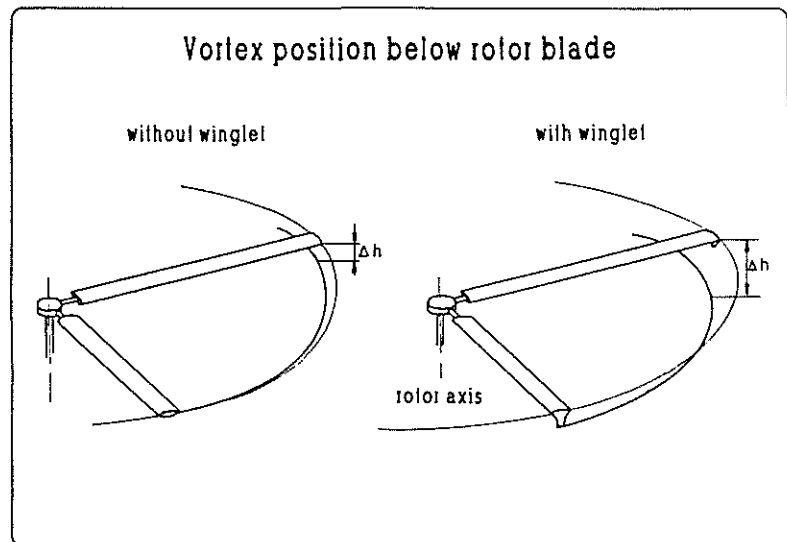


Fig. 2

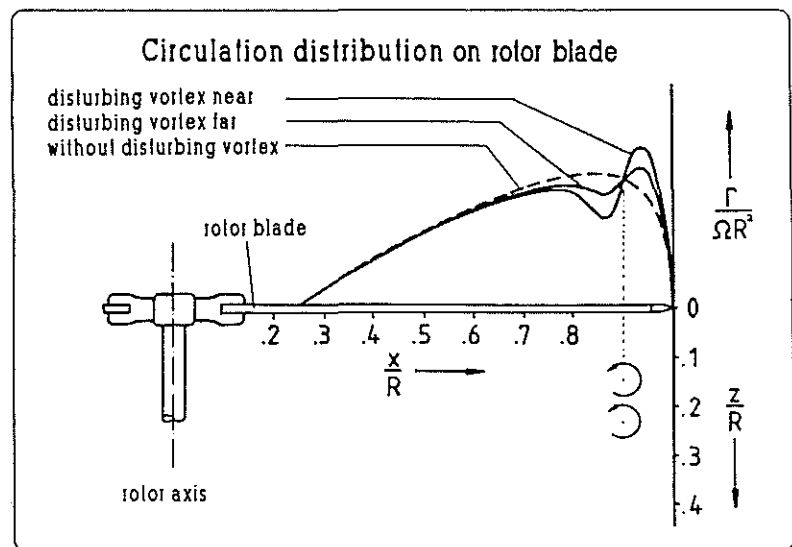


Fig. 3

which leads to a more or less strong gradient of the circulation distribution at the very tip. A larger angle of attack results in a larger vertical displacement of the vortex, but at the same time in a more concentrated vortex. In my investigation I have made experiments with a nontwisted winglet ( $0^\circ$ ) and a twisted winglet with a positive twist angle of  $7^\circ$  at the downward pointing part (Fig. 5). There is an additional angle of  $\Delta\vartheta = 2^\circ$  in Fig. 5 due to the basic angle of attack of the blade. Calculations in hover case showed an optimum of the twist angle at about  $4^\circ$  (see /2/). For forward flight experiments and comparisons between theory and experiment I have preferably used the twisted winglet ( $7^\circ$ ) (Fig. 6).

I made a theoretical and experimental investigation providing the opportunity to make comparisons with experiments at every important step of the calculation. First of all I decided that it is not necessary to develop a new theoretical wake determination method like the free wake analysis. I have determined the wake position by smoke experiments. It is very important to get an exact wake position, because the vertical position or displacement of the vortices in the wake is responsible for the strength of BVI. Any inaccuracy would influence all further calculations. While this experimental

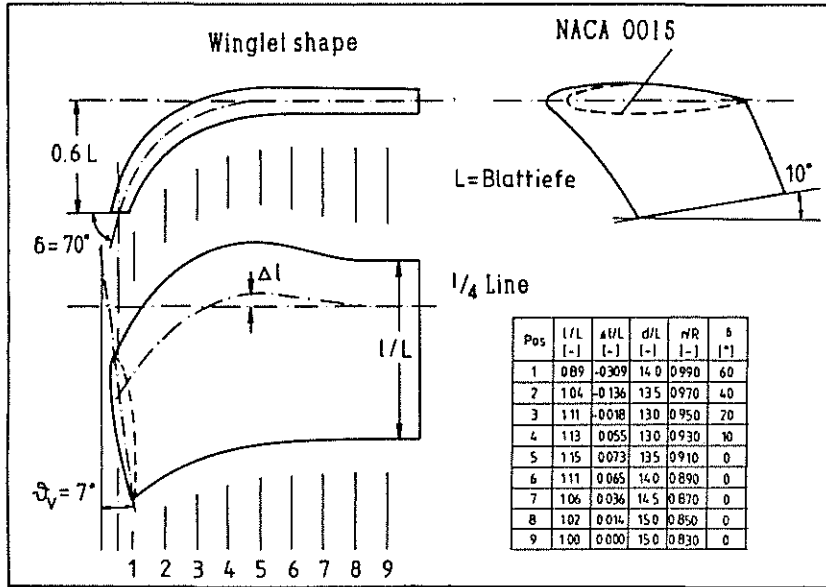
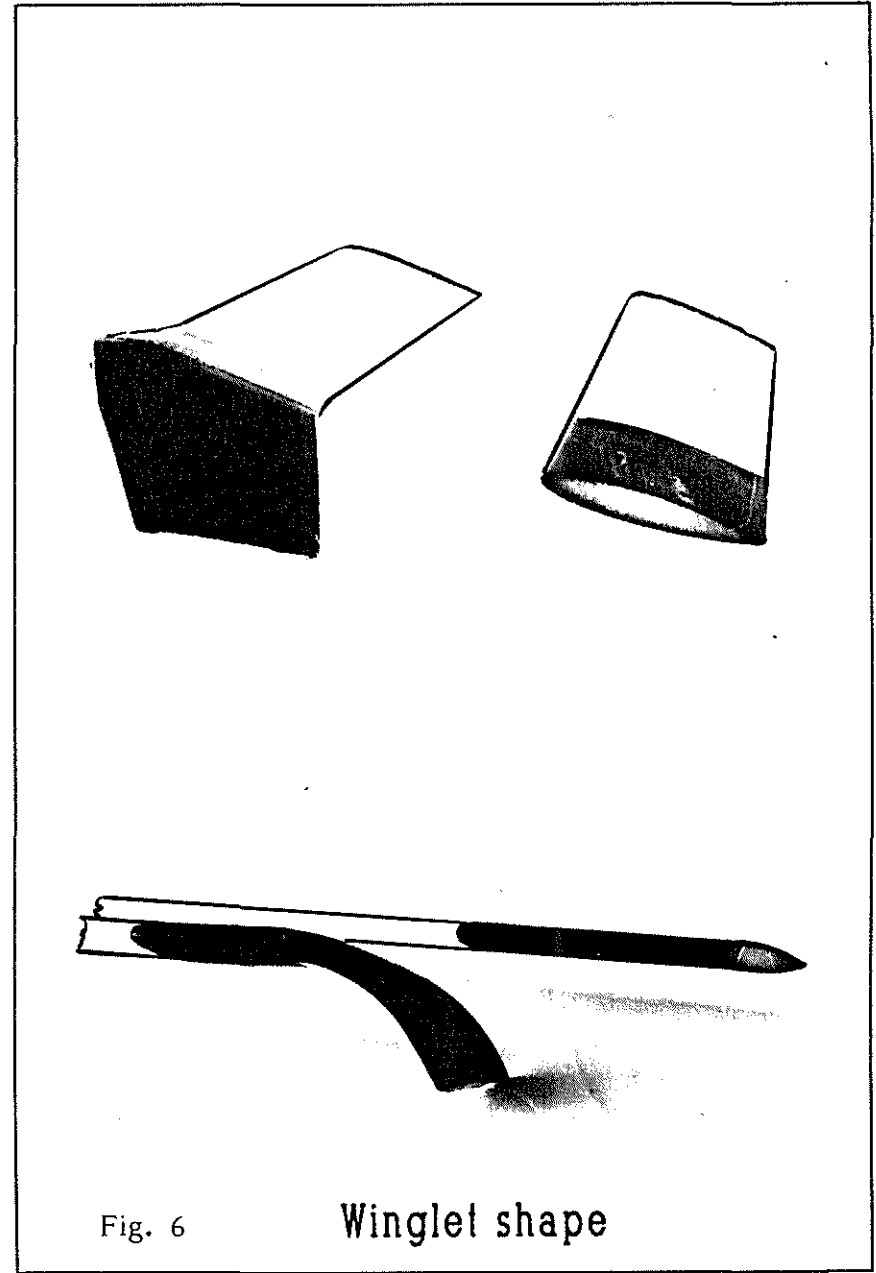
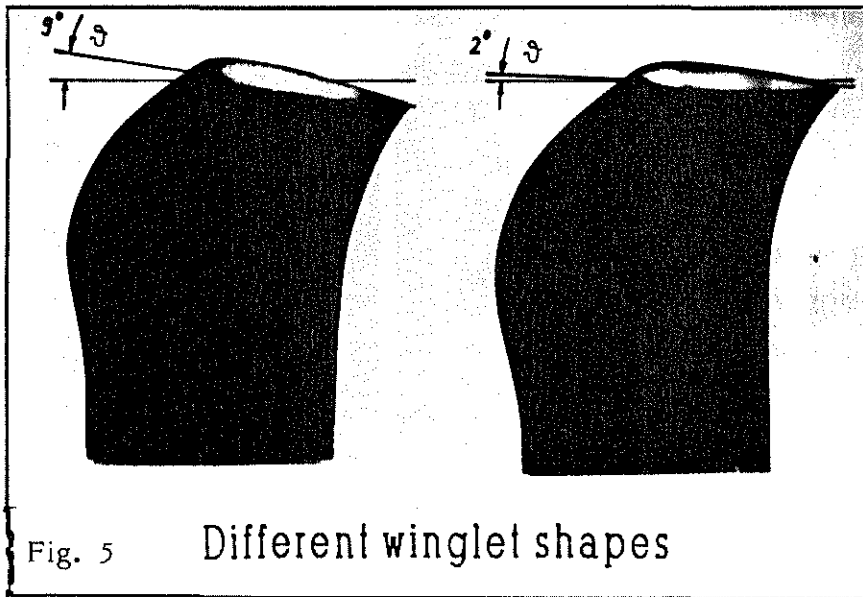


Fig. 4 Winglet shape



technique can be used for the investigation with the model rotor, it will be necessary to implement a full theoretical free wake analysis method for the extension to larger rotors. But I am sure that it is possible to adapt and extend the methods of Scully /4/ or Bliss /5/ to the problems of winglets.

## 2. EXPERIMENTS

As mentioned, the first and most important experiment was the determination of the rotor wake position. With an experimental setup (Fig. 7) equipped with two cameras and the visualization technique already shown in /1/ -- blowing vapour out of one of the blade tips -- it was possible to obtain vapour-photographs like Fig. 8. The quality of these photographs is not as high as shown in /1/ due to the higher rotor speed of 1500 RPM. Nevertheless it was possible to reconstruct the vortex path very accurately over 1.5 revolutions of the vortex spiral. Very helpful for this task was the observation of the wake development at different rotor azimuth (photographs were taken at  $10^\circ$ -steps) and a simultaneously recorded video tape. The measured vertical wake displacement was considerably (almost the winglet height). By means of digital picture processing methods it was possible to extract the center lines of the vapour filaments in the photographs and to obtain the position of the vortex core (Fig. 9). The superposition of the vortex spirals of all four blades shows the full wake (Fig. 10). This wake serves as an input for all further calculations of induced velocities, bound circulation, blade pressure and blade forces and finally the emitted sound pressure.

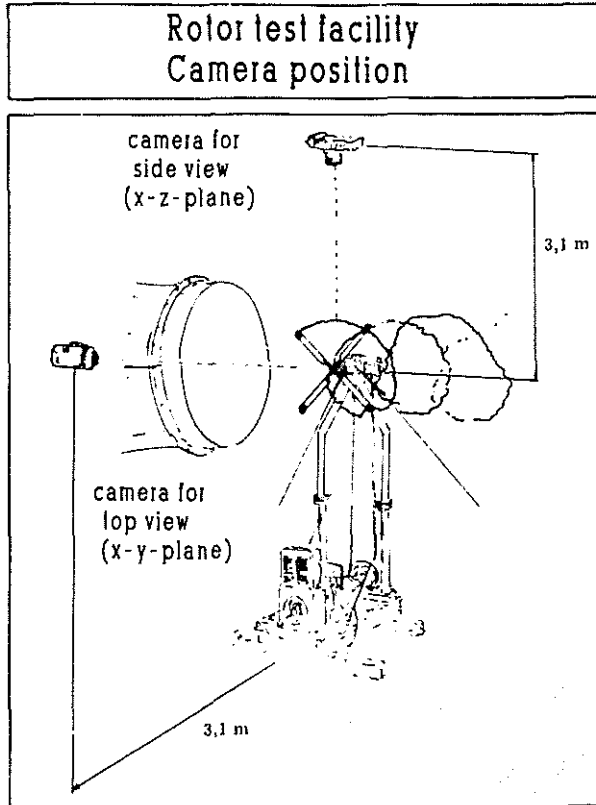


Fig. 7

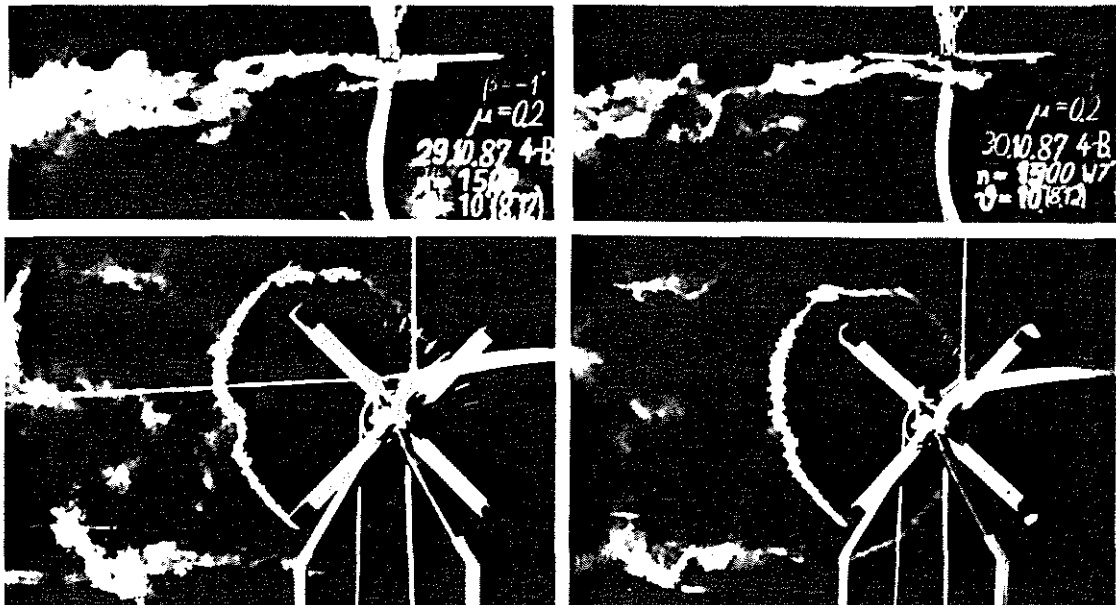


Fig. 8

Visualized wake - without

with winglet

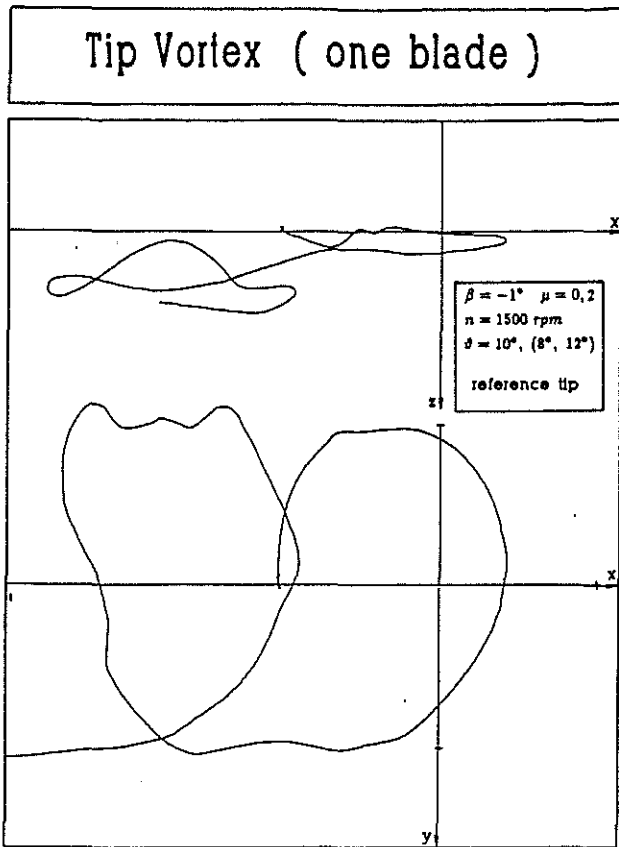


Fig. 9

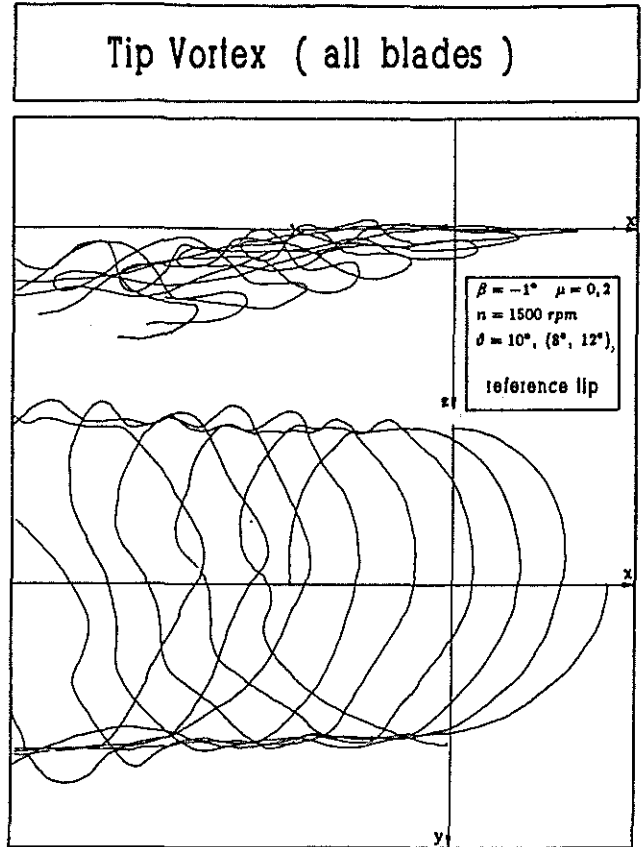
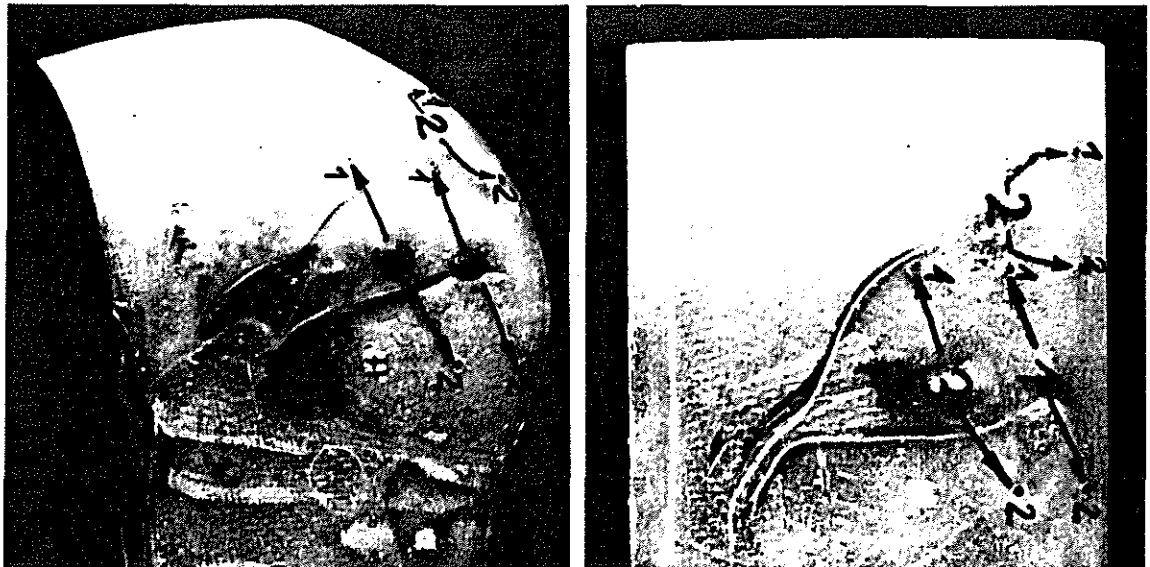


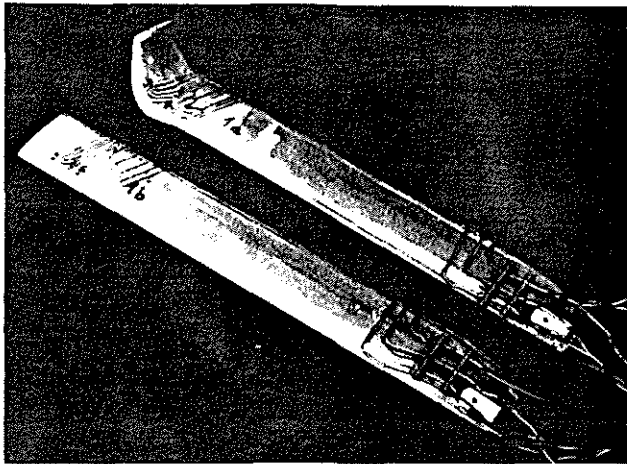
Fig. 10



Location of pressure probes

Fig. 11

For the measurements of the unsteady blade pressure a rectangular reference blade and a rotor blade with winglet were equipped with pressure probes (Fig. 11 and 12). These probes are located in the tip region at 90%, 95% and 97.5% radius and at different chord stations (5%, 20%, 40%), partly on the suction side and on the pressure side.



Rotor blades with pressure probes

Fig. 12

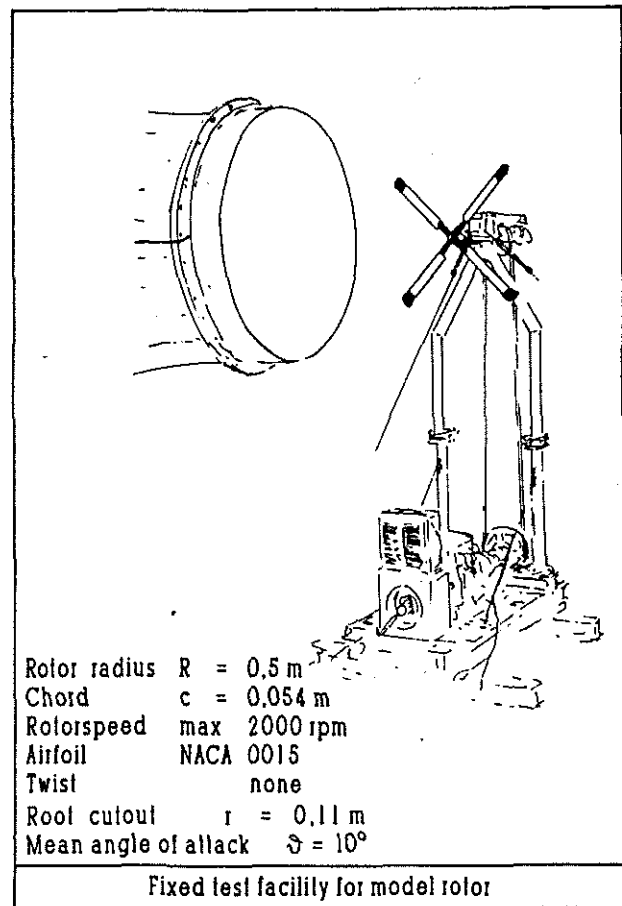


Fig. 13

The test rotor (Fig. 13) is equipped with a swashplate. So it was possible to perform the measurements at trimmed flight conditions. Actually it was not possible to set the trim absolutely correct during the measurements as can be seen from the pressure courses, but at least the trim was the same for both configurations with reference tip and winglet. Several measurements are shown in Figs. 14 and 15 for a descent flight condition at an advance ratio of  $\mu = 0.2$  and in Figs. 16 and 17 for a level flight at an advance ratio of  $\mu = 0.3$ . In these and all the following figures there is always plotted the unsteady part of the pressure course. It is evident that the pressure fluctuations at 90% radius are considerably lower for the winglet configuration due to the larger distance between vortex and blade and due to the diffuser vortex core at BVI near the 90° and 270°-position. This is true up to a radius of 95%. At 97.5% radius there are strong pressure fluctuations due to the forward flight speed, which causes large variations of the angle of attack on the outer winglet part. But again the peaks caused by BVI at 90° and 270° are lower. This behaviour is similar at an even higher advance ratio of up to  $\mu = 0.4$ .

The measurements of the noise emission conducted in the farfield show the power spectrum of the noise due to the characteristic of the windtunnel room (noise reflecting walls). By measurements in the nearfield of the rotor, however, it was possible to get information of the sound pressure. In this nearfield, which depends on the frequency measured, the direct sound pressure of the rotor outweighs the reflected noise from the windtunnel walls.

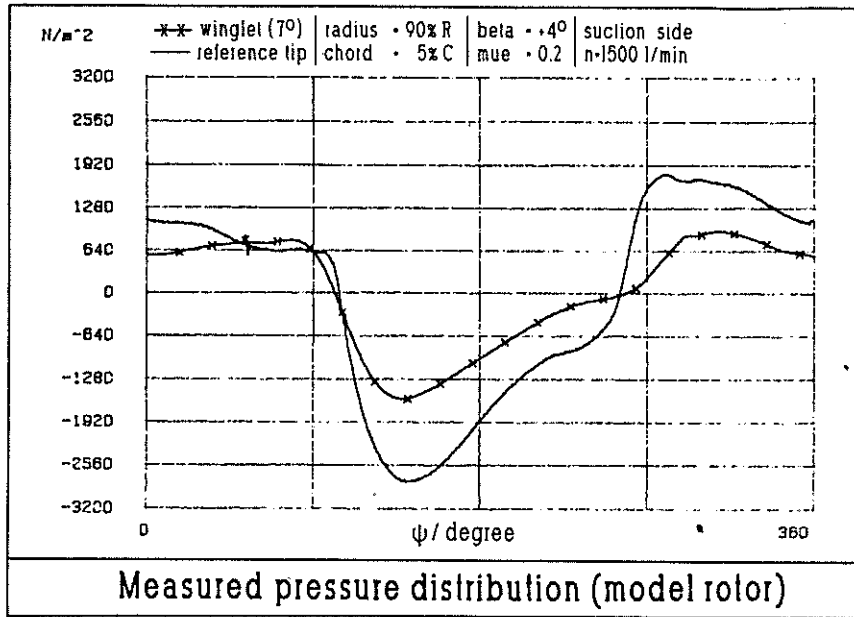


Fig. 14 Descending flight ( $\mu = 0.2$ )  $r/R = 0.9$

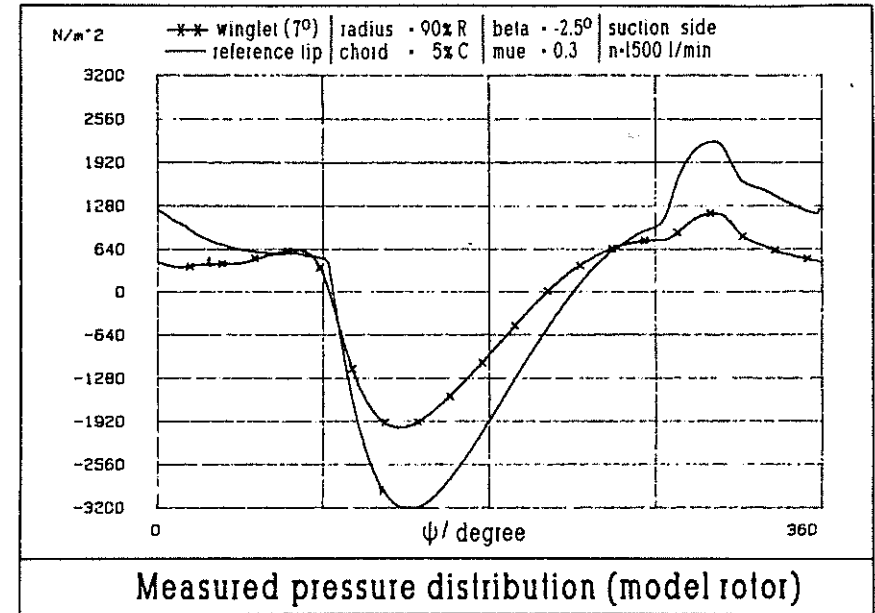


Fig. 16 Level Flight ( $\mu = 0.3$ )  $r/R = 0.9$

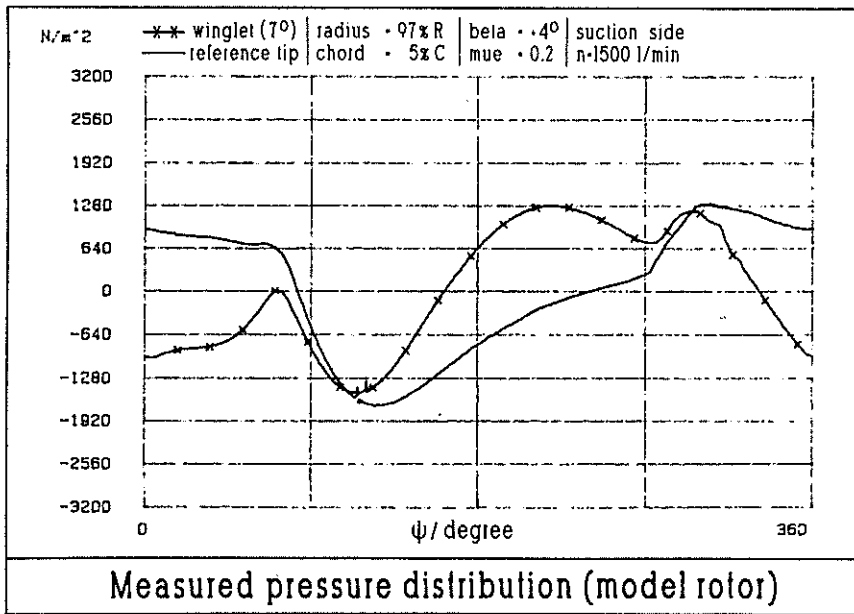


Fig. 15 Descending flight ( $\mu = 0.2$ )  $r/R = 0.975$

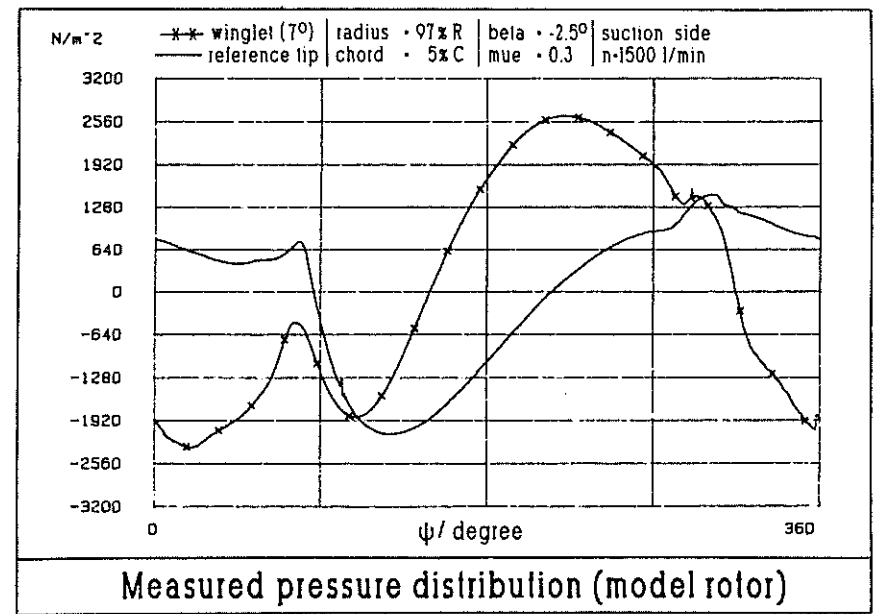


Fig. 17 Level flight ( $\mu = 0.3$ )  $r/R = 0.975$

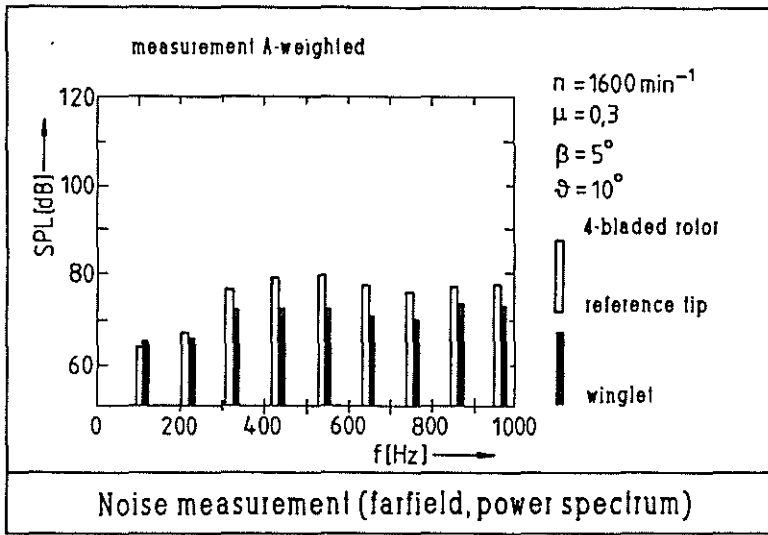


Fig. 18

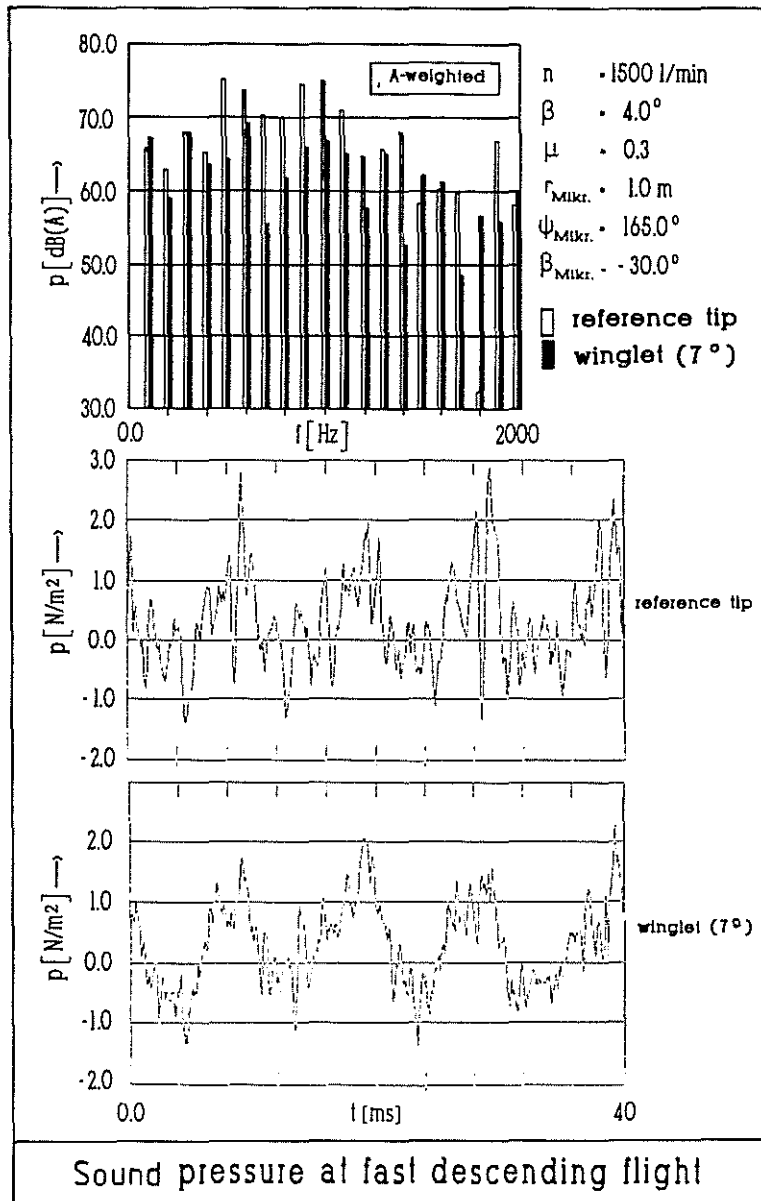


Fig. 19

An example of the farfield measurements is plotted in Fig. 18 for a very fast descent flight condition (A-weighted). The noise harmonics are considerably lower for the winglet configuration. A near-field measurement for a similar flight condition is shown in Fig. 19. Here the sound pressure is plotted in the time domain and in the frequency domain. The strong pressure peaks with the reference tip due to BVI are again considerably reduced by the winglet. In the frequency domain it is evident that most harmonics are up to 10dB(A) lower for the winglet configuration than for the rectangular reference tip.

### 3. THEORY

As mentioned in the introduction, the wake position (tip vortices) was determined with vapour photographs. The first step in the calculation was the determination of the induced velocities at the blade and the bound circulation distribution on the blade. To do this, the circulation distribution in the wake had to be known. Under the assumption that the tip vortices have the main effect within BVI, the circulation distribution in the tip vortex spirals could be calculated in an iterative process. Fig. 20 shows a flow chart of the program. In this process the blade is simulated by a vortex-lattice (Fig. 21). All induced velocities are calculated according to Biot-Savart. With these induced velocities and the boundary condition on the blade (profile contour) the vortex-lattice on the blade gives a set of equations. The solution of these equations is the bound circulation. The

calculation is done in azimuthal steps of  $\Delta\psi = 5^\circ$ . The circulation of the just developing tip vortex corresponds to the maximum bound vorticity on the blade (minus some loss of few percent). With this new circulation for the tip vortices a new iteration starts. The result at a moderate advance ratio of  $\mu = 0.2$  is plotted in Fig. 22. The circulation fluctuations at  $90^\circ$  and  $270^\circ$  azimuth are lower with the winglet. Fig. 23 shows the induced axial and tangential velocities at 80% radius. Again the distribution is smoother with the winglet.

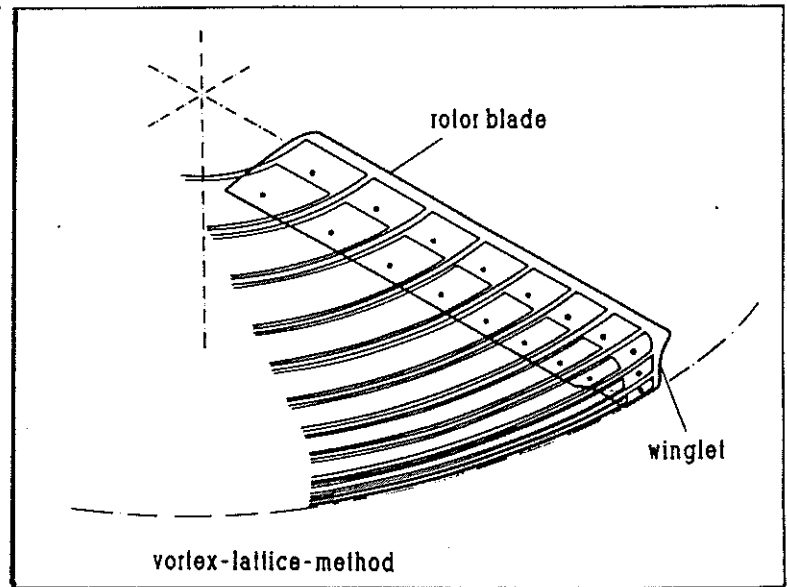


Fig. 20

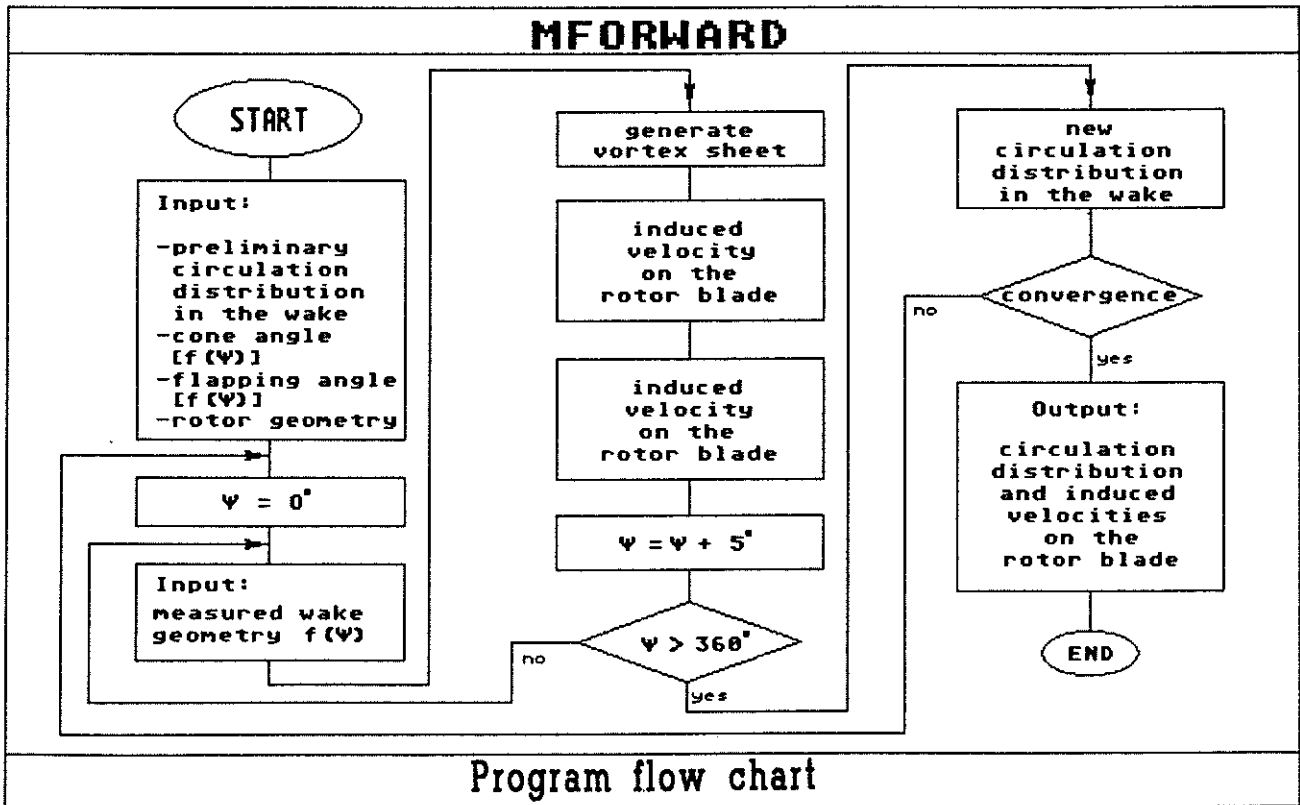


Fig. 21

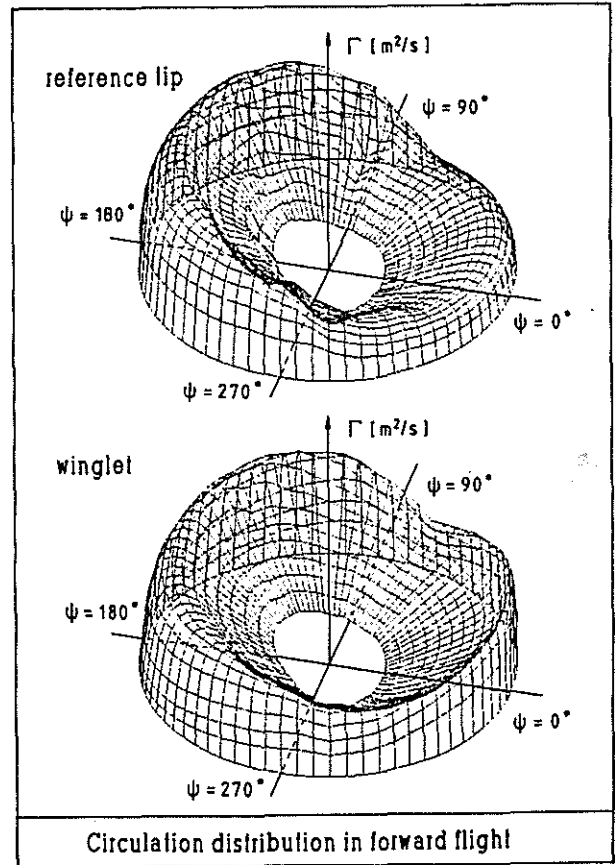
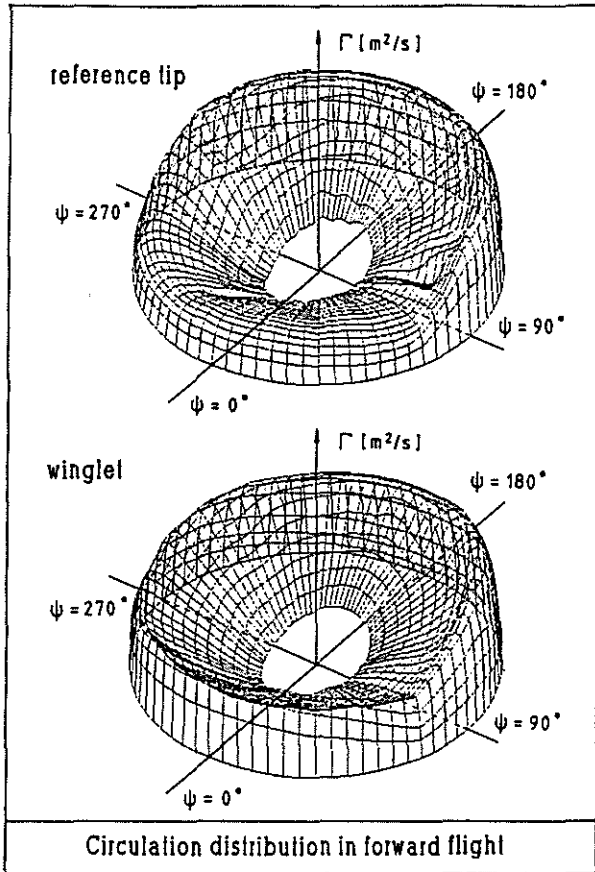


Fig. 22a,b

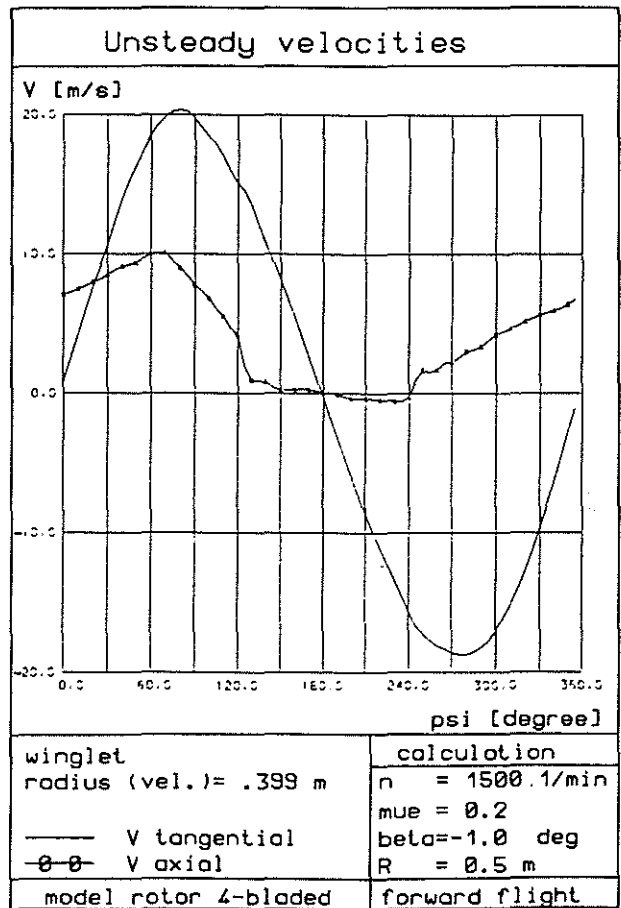
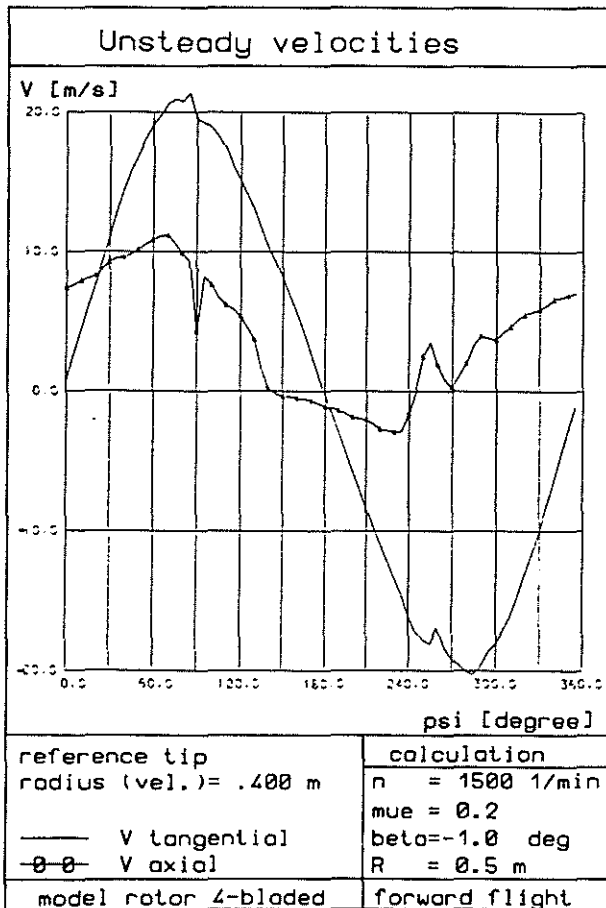


Fig. 23a,b

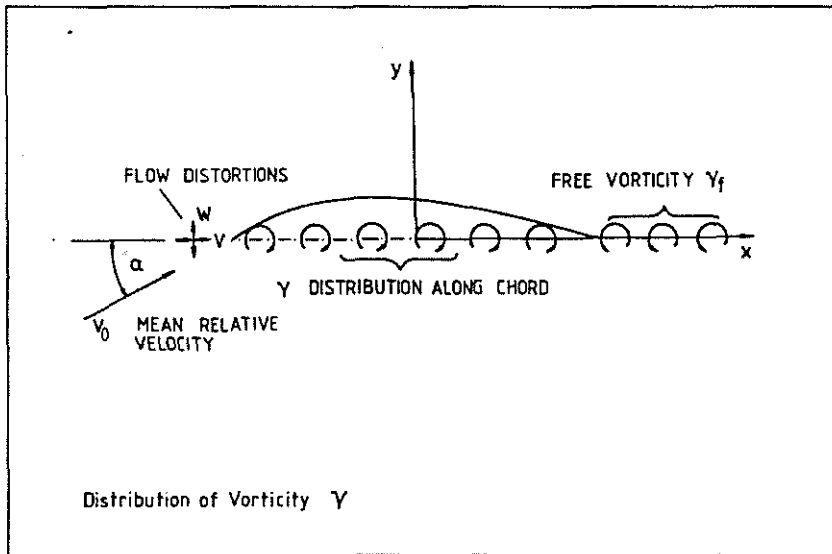


Fig. 24

With these induced velocities an unsteady pressure calculation has been performed using the approved method already shown in /1/ and /6/. In this theory the profile is represented by a 2-dimensional continuous circulation distribution (Fig. 24), which is influenced by the disturbing velocities  $u$  and  $v$ . These velocities again are influenced by variations of the angle of attack of the airfoil (cyclic control and flapping of the blade) and by BVI. Changes of the circulation distribution cause the development of free vorticity floating away with the free stream

velocity. Using this circulation distribution the velocities on the profile can be calculated according to Biot-Savart. With the one dimensional Euler equation, set up for the profile contour, integral equations for the unsteady pressure distribution can be constructed.

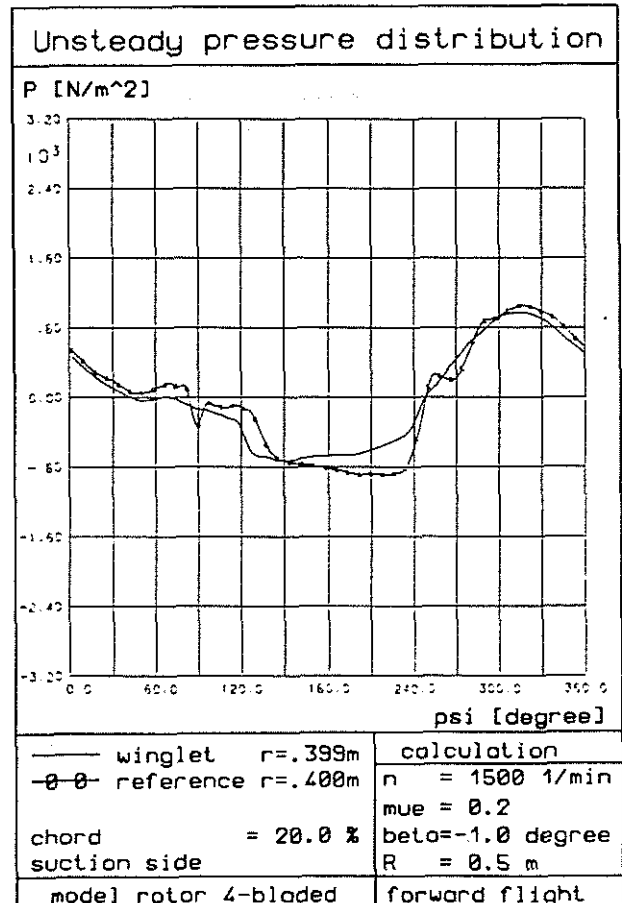
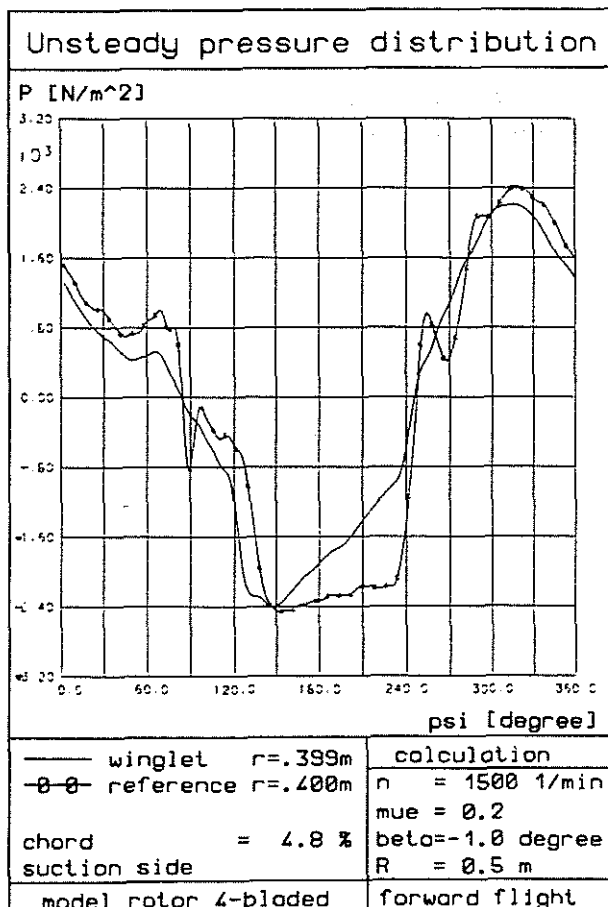


Fig. 25a,b

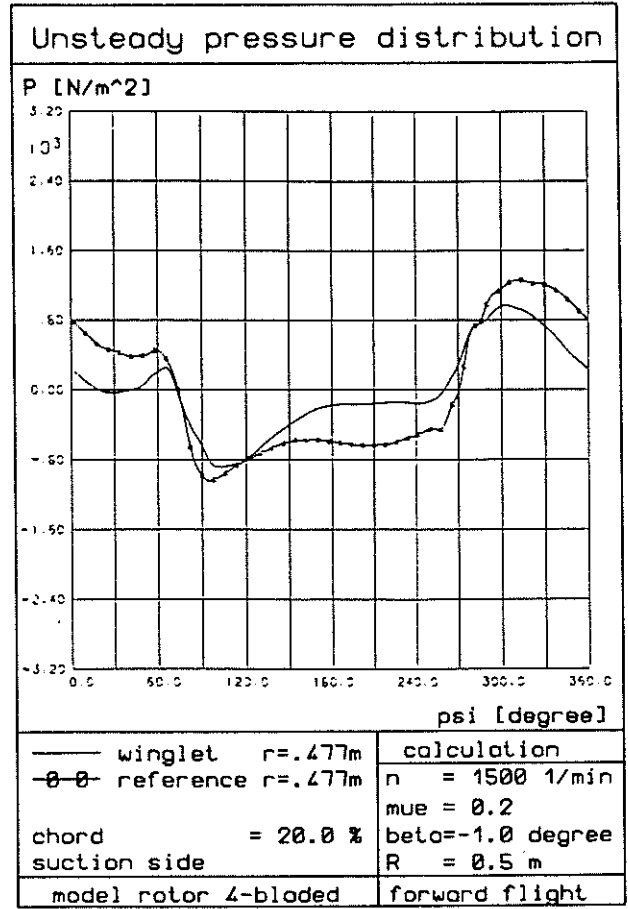
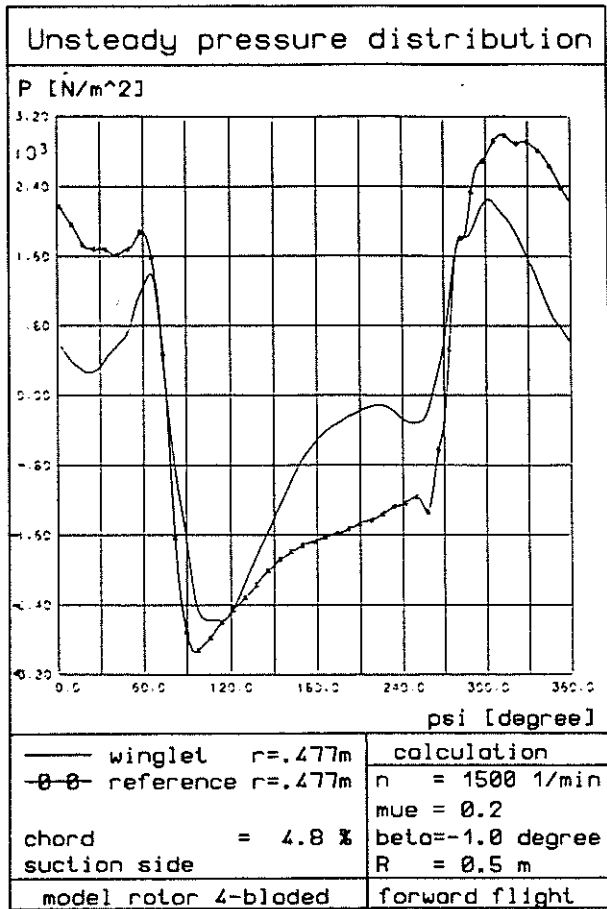


Fig. 26a,b

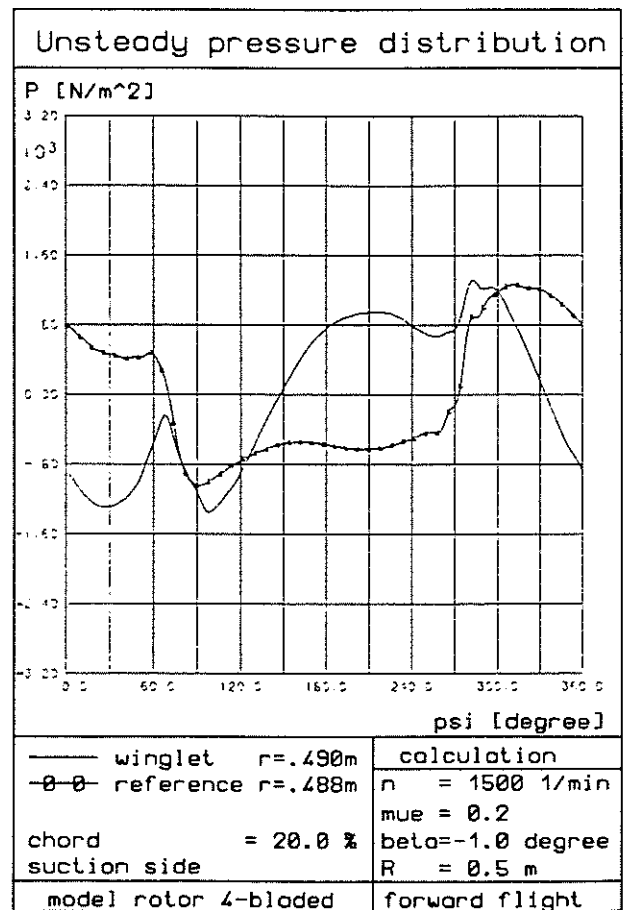
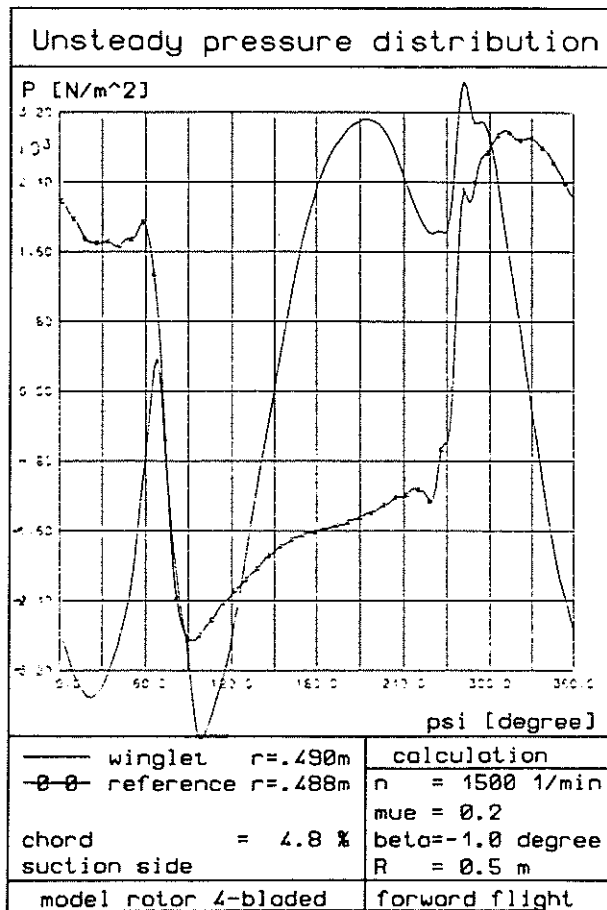


Fig. 27a,b

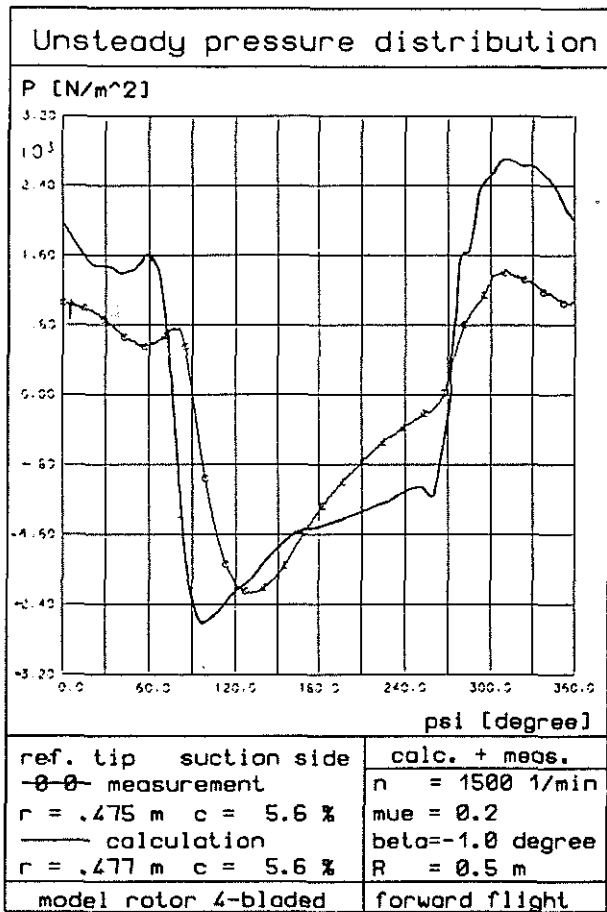
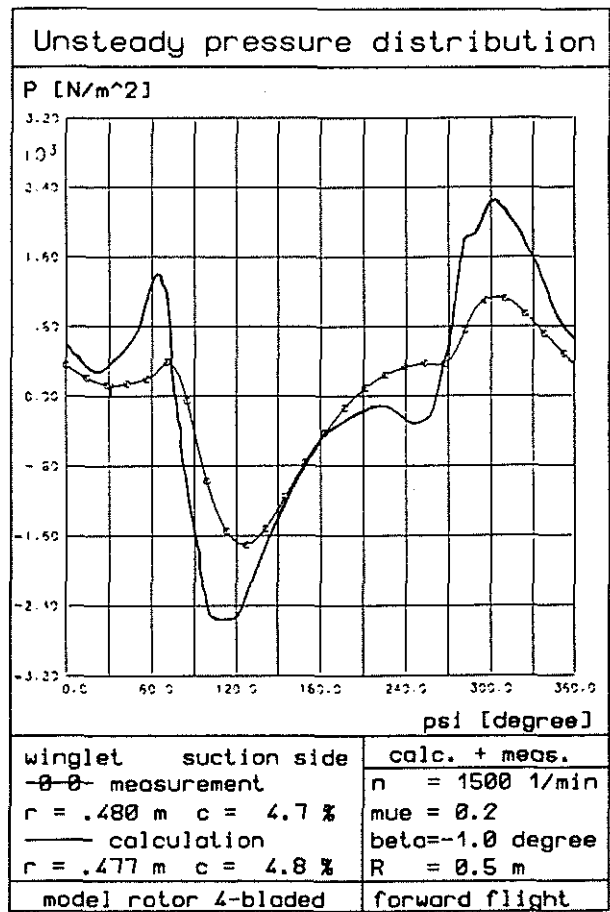


Fig. 28a,b  $r/R = 0.95$



$r/R = 0.95$

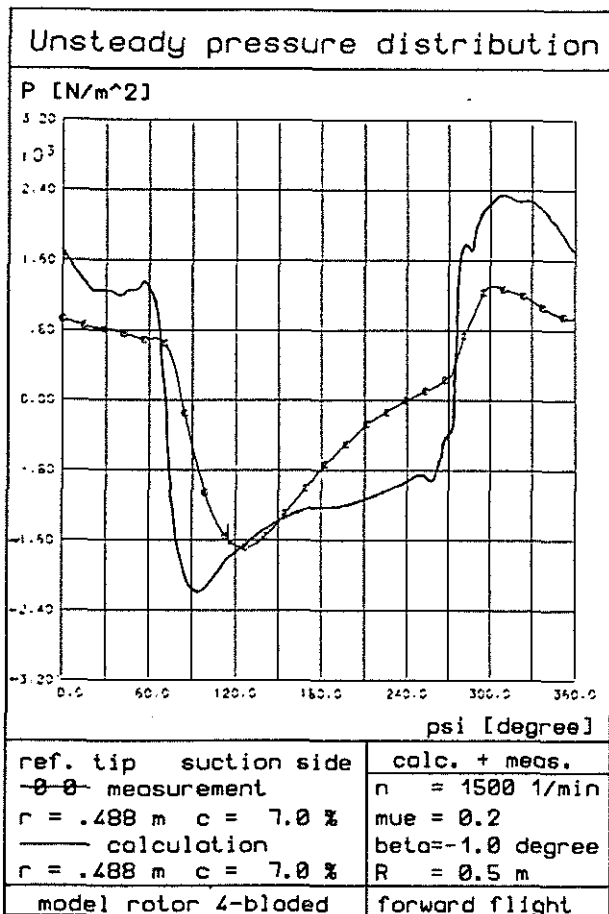
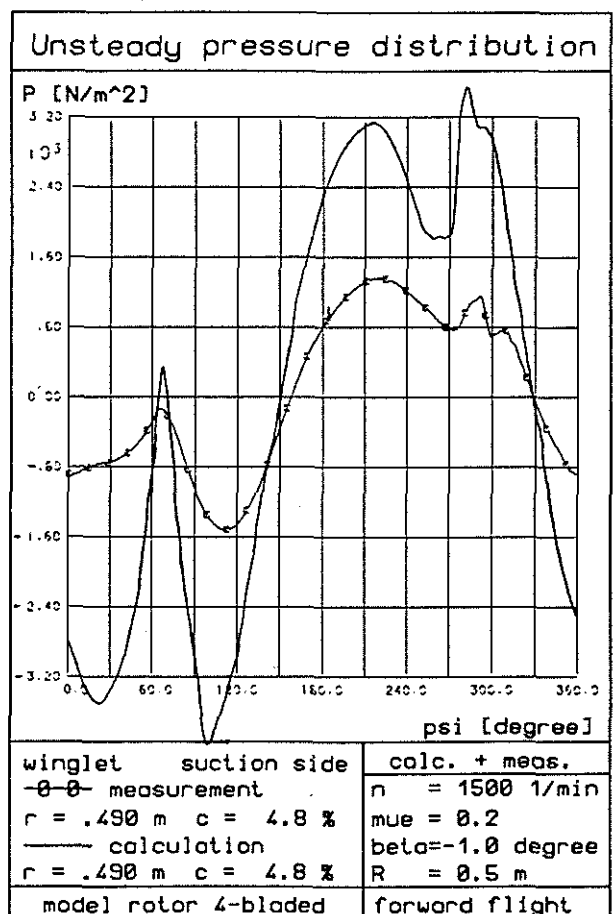


Fig. 29a,b  $r/R = 0.975$



$r/R = 0.975$

Results of this calculation are shown in Figs. 25 - 27 for the advance ratio of  $\mu = 0.2$  and a radius of 80%, 95% and 97.5%. The examples show the unsteady pressure course over one revolution for 5% and 20% chord. At 80% and 95% radius the influence of BVI is remarkably decreased by the winglet. At 97.5% radius -- on the winglet itself --, however, the influence of the strong variations of the angle of attack induced by the forward flight speed has an adverse effect. In Figs. 28 and 29 a comparison is made for theory and experiment for 95% and 97.5% radius. The agreement is only qualitatively good -- peaks caused by BVI have the same azimuthal positions. The calculated values however are too large by a factor of 1.5 to 2. There are two explanations to this problem:

- Only the determination of the BVI-induced disturbing velocities is 3-dimensional. The final calculation of the unsteady pressure is 2-dimensional. This theory is not necessarily very good especially at the bending of the winglet near 97.5% radius. It is interesting that just there the errors are at a maximum.
- There may be a vortex breakdown at BVI. Some visualization photographs showed such a vortex bursting (see /1/). A similar vortex bursting is assumed by Scully /4/ in his calculations.

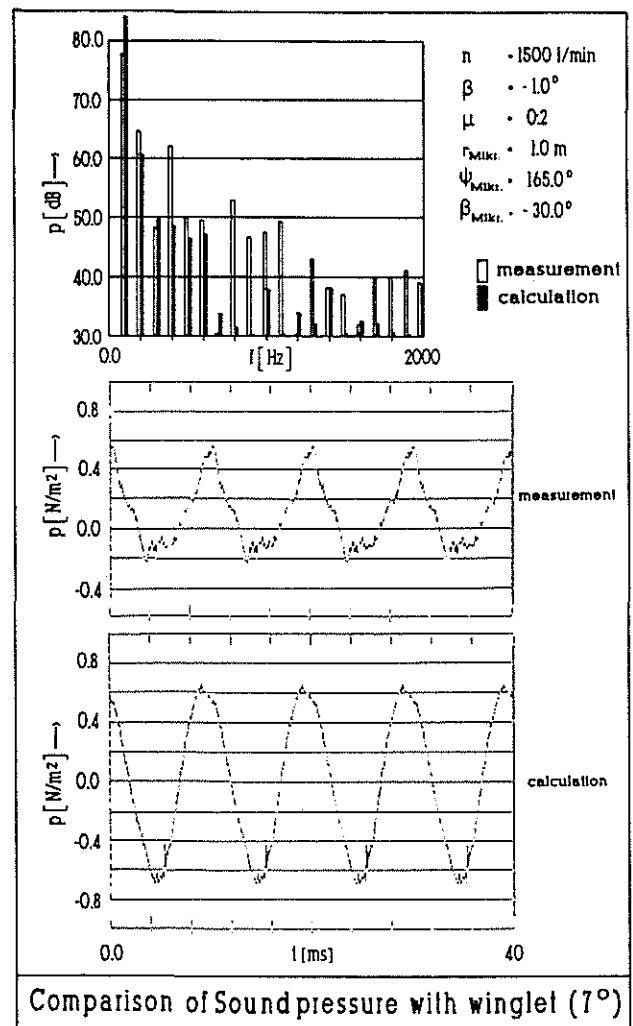
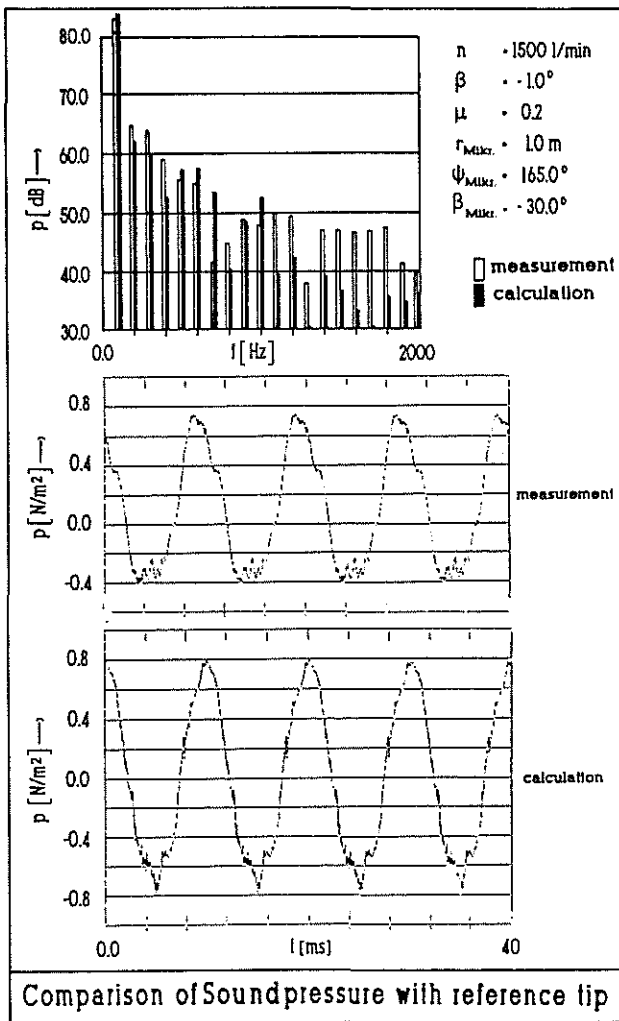


Fig. 30

Fig. 31

Calculations of the noise emission show a relatively good agreement up to the 10th harmonic with the reference tip (Fig. 30) and up to the 7th harmonic with the winglet (Fig. 31). These calculations use the Monopol and Dipol terms of the Ffowcs-Williams and Hawkins equation /7/, which was first adapted for the helicopter rotor by Schmitz and Yu /8/ and Schultz and Spletstoeser /9/. Schultz and Spletstoeser only use measured and interpolated pressure distributions on the rotor blades. On the other hand I have the possibility to use the measured and additionally -- at the locations where no measurements exist -- the calculated pressure distributions for this calculation of the sound pressure emitted by the rotor.

#### 4. SUMMARY

With both experiments and calculations the favourable influence of downward pointing winglets on the aerodynamic of helicopter rotors could be shown. Due to the increased vertical distance between tip vortex and rotor blades at BVI and due to a spreading of the vortex the unsteady pressure fluctuations on the blade are lower with the winglet. This results in lower blade stress and lower noise emission. Problems at higher forward flight speeds occur due to the strong azimuthal variations of the angle of attack on the winglet. These problems however can be overcome up to an advance ratio of  $\mu = 0.3$ . With these results a winglet arrangement will be very useful for heavy lift helicopters, where the increased efficiency of about 7% and even more (see /2/) will be substantial. Another important application of these winglets could be the tilt rotor helicopter. In this field there is no adverse influence of the winglets at higher forward flight speeds due to the symmetric flow conditions of the tilted rotors.

#### 5. ACKNOWLEDGEMENTS

This work was sponsored by the Deutsche Forschungsgemeinschaft (DFG) under the cooperative program SFB 25 (Sonderforschungsbereich 25). The author would like to thank U. Heinz and M. Lazik for the preparation of the figures.

#### 6. REFERENCE

- /1/ Müller, R.H.G.      The Influence of Winglets on Rotor  
    Staufenbiel, R.      Aerodynamics  
                            Vertica Vol 11, No 4, pp 601-618, 1987
- /2/ Müller, R.H.G.      Der Einfluß von Winglets an Rotorblattspitzen auf  
                            die Strömungsverhältnisse am Hubschrauberrotor  
                            Dissertation RWTH Aachen, July 1988, FRG  
                            to be published as:  
                            Fortschritt-Bericht VDI, Reihe 12 Nr. 108 (1988)
- /3/ Desopper, A.        Study of the Unsteady Transonic Flow on  
                            Rotor Blades with Different Tip Shapes  
                            Vertica, Vol 9, No.3, pp 257-272, 1985
- /4/ Scully, M.P.        Computation of Helicopter Rotor Wake  
                            Geometry and its Influence on Rotor  
                            Harmonic Airloads  
                            ASRL-TR-178-1, March 1975

- /5/ Bliss, D.B. Free Wake Calculations Using Curved  
 Teske, M.E. Vortex Elements  
 Quackenbush, T.R. Presented at the International Conference  
 on Rotorcraft Basic Research, Research  
 Triangle Park, North Carolina  
 February 19-21, 1985
- /6/ Neuwerth, G. Pressure Fluctuations on Rotor Blades  
 Müller, R.H.G. Generated by Blade Vortex Interactions  
 Vertica Vol.9 No 3 pp 227-239, 1985
- /7/ Ffowcs-Williams, J.E. Sound Generation by Turbulence  
 Hawkings, D.C. and Surfaces in Arbitrary Motion  
 Philos. Trans. R. Royce London  
 Ser. A. Vol 264, 1969
- /8/ Schmitz, F.H. Theoretical Modeling of High Speed  
 Yu, Y.H. Helicopter Impulsive Noise  
 3rd European Rotorcraft Forum  
 Aix en Provence, France, Sept. 7-9, 1977
- /9/ Schultz, K.-J. Prediction of Helicopter Rotor Impulsive  
 Splettsstoesser, W.R. Noise Using Measured Blade Pressures  
 43rd Annual Forum of the AHS  
 St. Louis, Missouri, May 1987